Large Protein-Induced Dipoles for a Symmetric Carotenoid in a Photosynthetic Antenna Complex

David S. Gottfried, Martin A. Steffen, Steven G. Boxer

Science, New Series, Volume 251, Issue 4994 (Feb. 8, 1991), 662-665.

_____ and P. D Harrison, *ibid.* **213**, 399 (1981); R. E. W. Adams, T. P. Culbert, W. E. Brown, Jr., P. D. Harrison, L. J. Levi, *J. Field Archaeol.* 17, 241 (1990); S. R. Gliessman, B. L. Turner II, R. May, M. F. Amador, in *Drained Field Agriculture in Central and South America*, J. P. Darch, Ed. (BAR International Series 189, Oxford Univ. Press, New York, 1983), pp. 91–110; V. L. Scarborough, in *ibid.*, pp. 123–136.
22. V. L. Scarborough, *Am. Antiquity* **48**, 720 (1983).
23. R. T. Matheny, *Science* **193**, 639 (1976).
24. C. P. Beetz and L. Satterthwaite, *The Monuments and Inscriptions of Caracol, Belize* (Univ. of Pennsylvania Press, Philadelphia, 1981); A. F. Chase and D. Z. Chase, *Investigation at the Classic Maya City of Caracol, Belize: 1985–1987* (Pre-Columbian Art Research Institute, San Francisco, 1987).
25. J. E. S. Thompson, *Excavations of San Jose, British Honduras* (Carnegie Institution of Washington, Washington, DC, 1939); T. H. Guderjan, *Archaeology*, in press.
26. P. A. McAnany, in *Precolumbian Population History in the Maya Lowlands*, T. P. Culbert and D. Rice, Eds. (Univ. of New Mexico Press, Albuquerque, in press); G. W. Brainerd, *Anthropological Records, Vol. 19* (Univ. of California Press, Berkeley, 1958). *Chultunes* that occur in the southern Maya Lowlands were probably not used to store water as they were in the more arid northern lowlands [see R. E. Reina and R. M. Hill, *Am. Antiq.* **45**, 74 (1980); B. H. Dahlin and W. J. Litzinger, *ibid.* **51**, 721 (1986).
27. Reservoirs at large centers represent "resource concentrations" [see R. F. Carneiro, *Science* **169**, 733 (1970)].
28. We thank B. L. Isaac, P. Mora, R. H. Halperin, K. Dejong, R. E. W. Adams, C. C. Coggins, N. Hammond, and T. P. Culbert for reviewing the manuscript. The University Museum, University of Pennsylvania, permitted the reproductions of the altered base maps. Support for this project was provided by the University Dean's Office as well as the Office of the Dean for Arts and Sciences at the University of Cincinnati.

27 September 1990; accepted 3 January 1991

Large Protein-Induced Dipoles for a Symmetric Carotenoid in a Photosynthetic Antenna Complex

DAVID S. GOTTFRIED, MARTIN A. STEFFEN, STEVEN G. BOXER

Unusually large electric field effects have been measured for the absorption spectra of carotenoids (spheroidene) in the B800–850 light-harvesting complex from the photosynthetic bacterium *Rhodobacter sphaeroides*. Quantitative analysis shows that the difference in the permanent dipole moment between the ground state and excited states in this protein complex is substantially larger than for pure spheroidene extracted from the protein. The results demonstrate the presence of a large perturbation on the electronic structure of this nearly symmetric carotenoid due to the organized environment in the protein. This work also provides an explanation for the seemingly anomalous dependence of carotenoid band shifts on transmembrane potential and a generally useful approach for calibrating electric field–sensitive dyes that are widely used to probe potentials in biological systems.

CAROTENOIDS ARE WIDELY DISTRIBUTED in nature and serve a wide range of functions (*1*). They are especially important in photosynthetic systems where they serve the dual functions of light harvesting and photoprotection (*2*). In addition to these important physiological roles of carotenoids, shifts in the absorption spectra of carotenoids have been widely used to measure transmembrane potentials and the electrogenicity of charge separation steps (*3*). Underlying the utility of these band shifts is quantitative information on the change in dipole moment, $\Delta\mu_A$, and the change in polarizability, $\Delta\alpha$, for these chromophores in their specific protein environment; to date, there is relatively little direct information on these essential properties. In the course of investigating the effects of applied electric fields on the absorption and emission spectra of bacteriochlorophyll a (BChl a) in photosynthetic antenna complexes (*4*), we examined the Stark effect spectrum in the region of the carotenoid absorption bands. Unusually large effects were observed, and these are shown to result from the interaction between the chromophore and the organized environment in the protein. The direct determination of electro-optic parameters for these polyene chromophores by Stark effect spectroscopy provides some of the quantitative basis needed for the evaluation of carotenoid band shifts under physiological conditions.

The B800–850 (LHII) antenna complex from purple nonsulfur bacteria such as *Rhodobacter sphaeroides* has been characterized in detail with respect to composition (*5, 6*), electronic absorption and emission spectroscopy (*7*), BChl a Stark effect spectroscopy (*4*), and energy transfer (*8*). This complex is the major pigment-bearing protein in the membranes of these organisms. Diffraction-quality crystals of B800–850 from different bacteria have been prepared by several groups (*9*), but a structure is not yet available. The complex consists of BChl a and carotenoid chromophores in a 2:1 ratio (*6*), which are complexed with a pair of α-helical transmembrane polypeptides (*10*). The chemical identity of the carotenoids present depends on the growth conditions: under anaerobic growth conditions, the dominant carotenoid is spheroidene; under semiaerobic growth conditions, spheroidenone accumulates with the exact fraction present dependent on the level of O_2 during cell growth (*11*).

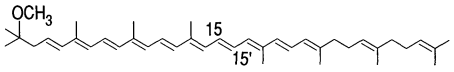

Spheroidene

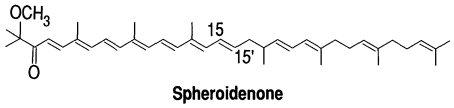

Spheroidenone

It is generally agreed that the carotenoids in the B800–850 complex are all-*trans* (*12*) and that their transition dipole moments, which are roughly parallel to the long molecular axis, lie approximately 45° to 50° away from the plane of the membrane (*13*). The carotenoids function both to transfer energy to the lower energy BChl a components and to quench potentially reactive and destructive BChl a triplet states, should they be formed (*2, 8*).

Stark effect spectroscopy can provide direct information on $\Delta\boldsymbol{\mu}_A$, $\Delta\boldsymbol{\alpha}$, and field-dependent changes in oscillator strength (due to transition polarizability and hyperpolarizability). If these effects are independent of each other, then for an immobilized isotropic sample, changes in dipole moment lead to band-broadening (second derivative–shaped features in the Stark effect spectrum), changes in polarizability lead to band shifts (first-derivative effects), and changes in oscillator strength produce zeroth and first-derivative effects (*14*). The apparatus for measurement of electric field effects and the determination of $|\Delta\boldsymbol{\mu}_A|$ and the angle ζ_A between $\Delta\boldsymbol{\mu}_A$ and the transition moment have been described (*15*).

All Stark effect spectra were found to scale quadratically with the externally applied electric field as expected for an isotropic, immobilized sample. Derivatives of the absorption spectra were obtained either directly from the data (generally smoothed with a Savitsky-Golay moving window or Fourier filtering) or the data were fitted to a combination of skewed Gaussian bands, followed by numerical differentiation. Contributions of zeroth, first, and second derivatives to the

Department of Chemistry, Stanford University, Stanford, CA 94305.

observed Stark effect spectrum (the ΔA spectrum) were then determined by a least-squares fit. The actual internal field felt by a chromophore due to the externally applied field, $\mathbf{F}_{ext}$, is denoted $\mathbf{F}_{int}$, where $\mathbf{F}_{int} = f\mathbf{F}_{ext}$, and f is the local field correction. An ellipsoidal cavity approximation has been shown to be appropriate for linear polyenes (*16, 17*). Since the difference dipole lies along the long axis of the molecule (see below), the major axis component of the local field correction tensor is relevant. For typical ellipsoidal cavity parameters for polyenes and solvent dielectric constants, this component is between 1 and 1.1 (*16, 17*). Values of $|\Delta\mu_A|$ are reported in units of Debye/f to facilitate comparison.

The absorption spectrum, Stark effect, and second derivative of the absorption spectrum in the carotenoid and BChl a Q_x region for the B800–850 antenna complex isolated from anaerobically grown (>95% spheroidene-containing) *Rb. sphaeroides* (wild-type strain 2.4.1) are shown in Fig. 1. The Stark effect for the absorption bands (origin and vibronic) of the carotenoid is huge (about 100 times that measured for the Q_x transitions of the BChl a chromophores around 600 nm). The absorption spectrum of spheroidene in the complex (Fig. 1A) shows a well-resolved series of vibronic bands. A prominent, second derivative–shaped Stark effect feature is observed for each band, including all of the shoulders on the bands (Fig. 1, B and C). The angle ζ_A between $\Delta\mu_A$ and the transition moment was found to be $\zeta_A = 10° \pm 2°$ and is the same for each vibronic component. Because of the excellent resolution of bands in the absorption spectrum and the close agreement of the Stark effect spectrum with the second derivative of the absorption, an accurate value $|\Delta\mu_A| = 15.3 \pm 0.7$ D/f was determined (*18*). Within the experimental uncertainty, this same value of $|\Delta\mu_A|$ was obtained for each vibronic component. There is little, if any, contribution attributable to a first-derivative line shape (this would be evident as a shift of the Stark features relative to the absorption features). A comparative study of spheroidene and spheroidenone in the B800–850 antenna complex and in wild-type and mutant reaction center complexes is presented elsewhere (*19*). In all cases the dominant feature of the Stark effect spectrum in the Q_x region (400 to 600 nm) arises from the carotenoid. Spheroidenone appears to be even more sensitive to electric fields than spheroidene (that is, it has a larger $|\Delta\mu_A|$) in all of the protein complexes examined; however, the line shape analysis is considerably more complex.

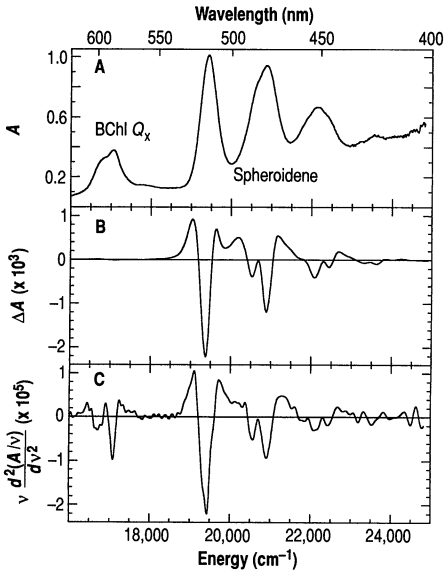

Fig. 1. (**A**) Absorption spectrum, (**B**) Stark effect, and (**C**) second derivative of the absorption spectrum of the B800–850 complex obtained from organisms grown under anaerobic conditions (spheroidene is the carotenoid). The sample is in a glycerol buffer (15 mM tris, 0.1% lauryldimethylamine oxide, pH. 8.0) glass at 77 K, $\mathbf{F}_{ext} = 1 \times 10^5$ V/cm, and the ΔA spectrum was obtained at the magic angle ($\chi = 54.7°$).

The absorption spectrum for pure spheroidene in poly(methyl methacrylate) (PMMA) is shown in Fig. 2A, the Stark effect spectrum in Fig. 2B, and the first and second derivatives of the absorption spectrum in Fig. 2, C and D, respectively. The ΔA spectrum has nearly the same shape as the first derivative except that it is shifted approximately 250 cm^{-1} to lower energy. The data (origin and all vibronic bands) can be fitted quite well by a sum of first-derivative and second-derivative contributions. This provides an upper limit for the value of $|\Delta\mu_A| < 4.7$ D/f and a lower limit for $|\mathrm{Tr}(\Delta\alpha)| > 500$ Å$^3/f^2$. The angle between $\Delta\mu_A$ and the transition moment was determined as $\zeta_A = 15° \pm 2°$, and the long axis of the polarizability tensor was also found to be approximately parallel to the direction of the transition moment (*20*).

The results presented here provide an extraordinary example of the degree to which an organized environment such as that found within a protein complex can affect the electronic structure of a bound chromophore. The observations for the B800–850 complex that the Stark effect line shape closely matches the second derivative of the absorption spectrum and that the entire vibronic progression can be fitted with a single value of $|\Delta\mu_A|$ and a single value of ζ_A demonstrate that the observed electrochromic effect is essentially entirely due to a change in permanent dipole moment between the ground and excited state, with no discernible contribution from changes in the polarizability, hyperpolarizability, or transition moment. Although the first derivative–shaped contribution due to $|\Delta\alpha|$ should be comparable in the Stark effect spectra of spheroidene in the protein and isolated in a nonpolar glass matrix, the large value of $|\Delta\mu_A|$ induced by the protein environment is so large that this contribution is not detectable. Interestingly, there is no evidence that there is any difference in the electronic structure of the three spheroidene molecules in the minimal unit of the antenna complex. This point is made especially clear by a comparison of the linewidths of the spheroidene absorption bands in the B800–850 complex and in PMMA. Given that there are three carotenoid molecules per minimal unit in the antenna complex (*7*) and that different chromophore orientations and positions could lead to differing transition energies, it is striking that the complex shows a narrower line shape than the PMMA film. This is consistent with a very well-structured environment in the vicinity of the carotenoid.

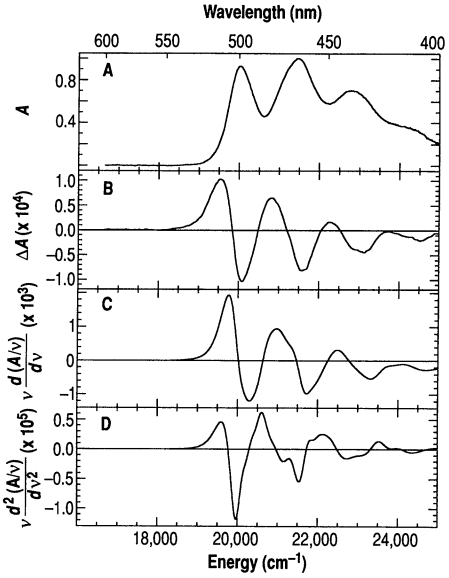

Fig. 2. (**A**) Absorption spectrum, (**B**) Stark effect, (**C**) first derivative of the absorption spectrum, and (**D**) second derivative of the absorption spectrum of spheroidene. The carotenoid is in a poly(methyl methacrylate) film at 77 K, $\mathbf{F}_{ext} = 1 \times 10^5$ V/cm, and the ΔA spectrum was obtained at the magic angle ($\chi = 54.7°$).

An obvious question is how can such a large difference in the permanent dipole moment be present for a chromophore as symmetric as spheroidene? Solvent-induced symmetry breaking (in this case the protein is the solvent) has been well documented in the chemical physics literature (*21*) and has been used to explain the large Stark effect for the special pair in the photosynthetic reaction center (*22*). The dependence of carotenoid band shifts on transmembrane potential (see below) indicates indirectly that it is

the difference in the dipole moment (induced by a large matrix field at the carotenoid binding site) that is responsible for the band shift (*23*). On the basis of the Stark effect data for the antenna complex, we see that this conclusion is correct. Polyenes are highly polarizable; that is, electric fields can induce substantial dipole moments. Several groups have investigated simple, centrosymmetric polyenes in organic solvents (*16, 21*). Relatively small, but nonzero, values of the apparent dipole moment difference were observed (1 to 4 D), along with large changes in polarizability. For a centrosymmetric molecule in the absence of solvent, $\Delta\mu_A$ should be zero; however, inhomogeneous local solvent interactions reduce the electronic symmetry and result in an apparent dipole moment (*21*). The situation in the B800–850 complex appears to be an extreme limit of this trend.

In the case of a Stark effect measurement of an isotropic sample, if the applied external field induces a dipole moment, then the induced dipole is effectively oriented, and the Stark effect spectrum has a first-derivative line shape (a band shift). Indeed, a substantial first-derivative component is observed for pure spheroidene in PMMA (Fig. 2), indicating a large contribution due to the change in polarizability. Thus, the Stark effect results for the protein complex demonstrate that matrix fields, whose relation to the carotenoid polarizability tensor is fixed by the structure of the carotenoid-protein complex, induce a substantial $\Delta\mu_A$, and these matrix fields must be substantially larger than the external field applied to make the Stark effect measurement. Spheroidene in the B800–850 complex is known to be all-*trans* with little evidence for any twisting (*12*). Consequently, its conformation in the protein is likely to be very similar to that in a PMMA matrix, yet $|\Delta\mu_A|$ is very different.

Kakitani *et al.* (*24*) have considered possible mechanisms that might lead to large induced dipole moments in carotenoids, focusing on effects of point charges from nearby amino acids. Model calculations suggest that point charges could provide a perturbation that would lead to large permanent dipole moments. Since a crystal structure is not yet available, it is too early to tell whether a specific point charge is the origin of the observed large value of $|\Delta\mu_A|$ or whether a constellation of partial charges, polar and polarizable groups, and helix dipoles in the protein collectively induce a permanent dipole in the carotenoid. It is known that the B800–850 antenna complex consists of an assembly of transmembrane helices associated with bacteriochlorophylls and carotenoids and that the long axis of the carotenoid is approximately 45° to the membrane normal (*13*). The approximate length of all-*trans* spheroidene is 40 Å; thus, it nearly spans the lipid bilayer. Consequently, it is quite possible that at one end the carotenoid is in close proximity to the bilayer surface and is near several potentially charged amino acids or polar lipid head groups. This is, in fact, the conclusion reached by Symons and Swysen (*25*) on the basis of the sensitivity of carotenoid band shifts in *Rb. capsulatus* to pronase treatment.

The observation that the spectra of carotenoids undergo shifts in response to changes in transmembrane potential and light-induced charge separation steps was first made in the mid-1950s (*26*). Several research groups have used light, ionic gradients, and electric fields to introduce transmembrane potentials. They then monitored the kinetics of spectral changes and measured the carotenoid difference spectra in order to determine a precise mechanism for the band shifts (*27–29*). In the absence of direct information on $\Delta\mu_A$, which is provided in this report, various indirect approaches were taken to determine the origin of the shift and to calibrate its response. One of the most important observations that has been made previously is that the band shift is approximately linear with respect to the apparent transmembrane potential (*27, 30*). In a native biological membrane, the carotenoid has a unique and fixed orientation with respect to the external field direction due to the transmembrane potential (the sample is uniaxially oriented with respect to the applied field). If $\Delta\mu_A$ is responsible for the band shift, one predicts a linear field dependence and first-derivative shape (band shift) because the change in transition energy is simply the product of the field strength with the projection of $\Delta\mu_A$ on the field direction (*31*). If $\Delta\alpha$ is responsible for the band shift, it should be quadratic in the applied field. For our immobilized isotropic samples, all orientations of $\Delta\mu_A$ are present relative to the external applied field with the result that shifts to both higher and lower energy occur, and the Stark effect is expected and observed to be quadratic with field, despite the fact that the interaction is identical to that for a uniaxially oriented sample. A quadratic field dependence is expected for an isotropic sample regardless of whether $\Delta\mu_A$ or $\Delta\alpha$ is responsible for the effect, provided that the Stark shift or splitting is less than the inhomogeneous linewidth; however, these are easily distinguished because $\Delta\mu_A$ and $\Delta\alpha$ give different line shape contributions to ΔA, as discussed above. In the early literature it was unclear if the applied transmembrane potential actually translated into an equivalent field strength across the bilayer and if contributions from $\Delta\mu_A$, $\Delta\alpha$, and changes in oscillator strength might conspire to give a linear field dependence (*3*).

The data in Fig. 1 show unambiguously that effects due to $\Delta\mu_A$ completely dominate all other effects in the B800–850 complex (*32*). Thus, the observed linear dependence on transmembrane potential in a uniaxially oriented sample is precisely what is expected. Furthermore, when quantitative information on $\Delta\mu_A$ is available from Stark effect measurements for each type of carotenoid and complex (*19*), band shift data can be translated into information on transmembrane potentials and electrogenicity with greater confidence.

REFERENCES AND NOTES

1. T. Goodwin and G. Britton, in *Plant Pigments*, T. W. Goodwin, Ed. (Academic Press, London, 1988), pp. 61–132; W. Rau, *ibid.*, pp. 231–255.
2. R. J. Cogdell and H. A. Frank, *Biochim. Biophys. Acta* **895**, 63 (1987).
3. C. A. Wraight, R. J. Cogdell, B. Chance, in *The Photosynthetic Bacteria*, R. K. Clayton and W. R. Sistrom, Eds. (Plenum, New York, 1978), pp. 471–511.
4. D. S. Gottfried, J. W. Stocker, S. G. Boxer, in preparation.
5. R. J. Cogdell and A. P. Crofts, *Biochim. Biophys. Acta* **502**, 409 (1978).
6. M. B. Evans, R. J. Cogdell, G. Britton, *ibid.* **935**, 292 (1988).
7. H. J. M. Kramer, R. van Grondelle, C. N. Hunter, H. H. J. Westerhuis, J. Amesz, *ibid.* **765**, 156 (1984).
8. J. K. Trautman *et al.*, *Proc. Natl. Acad. Sci. U.S.A.* **87**, 215 (1990).
9. J. P. Allen, R. Theiler, G. Feher, in *Antennas and Reaction Centers of Photosynthetic Bacteria*, M. E. Michel-Beyerle, Ed. (Springer-Verlag, Berlin, 1985), pp. 82–84; R. J. Cogdell *et al.*, *ibid.*, pp. 85–87; W. Mantele, K. Steck, T. Wacher, W. Welte, *ibid.*, pp. 88–91.
10. H. Zuber, *Trends Biochem. Sci.* **11**, 414 (1986).
11. D. Siefermann-Harms, *Biochim. Biophys. Acta* **811**, 325 (1985).
12. H. Hayashi, T. Noguchi, M. Tasumi, *Photochem. Photobiol.* **49**, 337 (1989).
13. J. Breton and E. Nabedryk, *Top. Photosynth.* **8**, 159 (1987).
14. W. Liptay, in *Excited States*, E. C. Lim, Ed. (Academic Press, New York, 1974), pp. 129–229; R. Mathies and L. Stryer, *Proc. Natl. Acad. Sci. U.S.A.* **73**, 2169 (1976). Mathies and Stryer observed a substantial value of $|\Delta\mu_A|$ for retinal in rhodopsin. Retinal is much less symmetric than spheroidene, and the symmetry is further lowered by the Schiff's base linkage to the protein.
15. D. J. Lockhart and S. G. Boxer, *Biochemistry* **26**, 664 (1987); *ibid.*, p. 2958; *Proc. Natl. Acad. Sci. U.S.A.* **85**, 107 (1988).
16. M. Ponder and R. Mathies, *J. Phys. Chem.* **87**, 5090 (1983).
17. A. Myers and R. Birge, *J. Am. Chem. Soc.* **103**, 1881 (1981).
18. Large nonlinear optical properties are likely to accompany these large values of $|\Delta\mu_A|$.
19. D. S. Gottfried, M. A. Steffen, S. G. Boxer, in preparation.
20. Fields of up to 10^6 V/cm were applied to spheroidene-PMMA samples in attempts to locate the 2^1A_g state, whose transition from the ground state is not observed in absorption because it is symmetry-forbidden. Although it is possible that a large electric field could enhance detection of this transition in the Stark spectrum (by state mixing, for example), no new features were observed in the spectral range 400 to 800 nm.
21. W. Liptay, R. Wortmann, R. Bohm, N. Detzer,

Chem. Phys. **120**, 439 (1988).
22. S. G. Boxer, R. A. Goldstein, D. J. Lockhart, T. R. Middendorf, L. Takiff, *J. Phys. Chem.* **93**, 8280 (1989).
23. R. Reich and S. Schmidt, *Ber. Bunsenges. Phys. Chem.* **76**, 589 (1972).
24. T. Kakitani, B. Honig, A. R. Crofts, *Biophys. J.* **39**, 57 (1982).
25. M. Symons and C. Swysen, *Biochim. Biophys. Acta* **723**, 454 (1983).
26. B. Chance and L. Smith, *Nature* **175**, 803 (1955); B. Chance, *Brookhaven Symp. Biol.* **11**, 74 (1958).
27. J. B. Jackson and A. R. Crofts, *FEBS Lett.* **4**, 185 (1969).
28. R. Reich, R. Scheerer, K.-U. Sewe, H. T. Witt, *Biochim. Biophys. Acta* **449**, 285 (1976); B. G. de Grooth and J. Amesz, *ibid.* **462**, 237 (1977); B. G. de Grooth, H. J. van Gorkom, R. F. Meiburg, *ibid.* **589**, 299 (1980).
29. M. Symons *et al.*, *ibid.* **462**, 706 (1977).
30. W. Junge and J. B. Jackson, in *Photosynthesis.* Vol. 1, *Energy Conservation in Plants and Bacteria*, Govindjee, Ed. (Academic Press, New York, 1982), pp. 589–646; W. Crielaard, K. J. Hellingwerf, W. N. Konings, *Biochim. Biophys. Acta* **973**, 205 (1988).
31. Samples that are artificially oriented by insertion into a lipid bilayer or in a Langmuir-Blodgett film are typically oriented axially, not uniaxially, relative to a unique field direction defined by a transmembrane potential. Hence, two populations with chromophore dipole moments having projections parallel and antiparallel to the field are present. So long as $\Delta\mu_A \cdot F_{int}$ (the Stark splitting) is comparable to or smaller than the inhomogeneous linewidth (nearly always the case), then ΔA should depend quadratically on the applied field if equal parallel and antiparallel orientational populations are present (D. J. Lockhart and S. G. Boxer, unpublished results). An isotropic sample is just the extension to all possible parallel and antiparallel orientational populations.
32. An interesting complication could arise if the applied field due to the transmembrane potential or charge separation reaction affected the distribution of matrix fields that induce the permanent dipole moment difference in the carotenoid.
33. We thank H. Frank and C. Violette for providing samples and advice, which were indispensable to this work. This work was supported by a grant from the National Science Foundation Biophysics Program. M.A.S. is a Medical Scientist Training Program (NIH) trainee supported by grant GM07365 from the National Institute of General Medical Sciences.

25 July 1990; accepted 12 October 1990

Fibroblast Growth Factor Receptors from Liver Vary in Three Structural Domains

JINZHAO HOU, MIKIO KAN, KERSTIN MCKEEHAN, GEORGE MCBRIDE, PAMELA ADAMS, WALLACE L. MCKEEHAN*

Changes in heparin-binding fibroblast growth factor gene expression and receptor phenotype occur during liver regeneration and in hepatoma cells. The nucleotide sequence of complementary DNA predicts that three amino-terminal domain motifs, two juxtamembrane motifs, and two intracellular carboxyl-terminal domain motifs combine to form a minimum of 6 and potentially 12 homologous polypeptides that constitute the growth factor receptor family in a single human liver cell population. Amino-terminal variants consisted of two transmembrane molecules that contained three and two immunoglobulin-like disulfide loops, as well as a potential intracellular form of the receptor. The two intracellular juxtamembrane motifs differed in a potential serine-threonine kinase phosphorylation site. One carboxyl-terminal motif was a putative tyrosine kinase that contained potential tyrosine phosphorylation sites. The second carboxyl-terminal motif was probably not a tyrosine kinase and did not exhibit the same candidate carboxyl-terminal tyrosine phosphorylation sites.

THE HEPARIN-BINDING FIBROBLAST growth factor (HBGF) family consists of seven related gene products that have a broad spectrum of biological effects on growth and function of a variety of cell types (*1*). Indirect ligand affinity chromatography and immunochemical analyses suggest that transmembrane tyrosine kinase–like molecules similar to the platelet-derived growth factor and the colony-stimulating factor one (*fms*) receptor family [*fms*-like genes (*flg*)] function as HBGF receptors (*2, 3*). HBGF stimulates and inhibits proliferation and secretory functions of cultured rat hepatocytes and differentiated human hepatoma cells. These cells exhibit a heterogeneous population of HBGF receptors with varied affinity for ligand (*4, 5*). Specific forms of the HBGF receptor may be responsible for a subset of the biological effects induced by the HBGF family members. Here we deduce, from the nucleotide sequence of cDNA, the structural features that combine to define a family of HBGF receptors in human liver cells.

We screened 2×10^6 plaques from a λgt11 expression library made from human hepatoma cell (HepG2) mRNA (*4*). Screening was conducted with synthetic oligonucleotide probes designed from the sequence of a partial human endothelial cell *flg* cDNA (*6*) and yielded five positive clones. Two 2.6-kb cDNAs, a1 and b2 (Fig. 1A), were 98% and 93% similar in nucleotide and deduced amino acid (aa) sequence, respectively (Fig. 1B). The a1 clone had a type 1 COOH-terminus and was identical to the partial human endothelial *flg* cDNA (*6*), except for a single base pair substitution (T to C), which caused a Val to Ala change in an extracellular immunoglobulin (IgG)-like loop structure (Fig. 1). The b2 clone differed from *flg* by a 6-bp (AACAGT) (2 aa) deletion in the intracellular juxtamembrane domain, and by a 25-bp insertion (GTGTGGAACCTGAAGGCTCCCCTGG) in the coding sequence for the second kinase consensus sequence in the intracellular domain (Fig. 1, type 2 COOH-terminus). The 25-bp insertion in b2 caused a shift in the reading frame, which produced a short second kinase consensus sequence (24 aa) followed by 44 unique COOH-terminal residues (Fig. 1). The juxtamembrane sequences encoded in the truncated *flg* cDNAs were designated as a (RRQVTVSA) and b (RRQVSA), respectively. The a and b motifs differed in a possible site of phosphorylation by a Ser-Thr protein kinase.

To deduce the NH_2-terminal sequences of *flg*-related gene products from HepG2 cells, we generated a sublibrary of primer-extended cDNA clones in λgt11 with a mixture of 3′-oligonucleotide primers common to a1 and b2 cDNAs (*7*). From the deduced aa sequences of the primer-extended cDNAs, we identified the NH_2-terminal (extracellular) motifs, which contained three (α) and two (β) IgG-like disulfide loops (Fig. 1). The polymerase chain reaction (PCR) (*8*) was used to further characterize heterogeneity in *flg*-related mRNAs in HepG2 cells [see Fig. 1B and (*9*) for primers]. The PCR was carried out with HepG2 first-strand cDNA as the template, a 5′ primer (P1a), which began 67-bp upstream of the common translational initiation site in the α and β cDNAs, and a 3′ primer (P1b), which ended 111-bp downstream from the first 3′ landmark (T/C) that distinguished a1 and b2 cDNAs (Fig. 1A). This yielded cDNA fragments of 1.1, 1.0, and 0.8 kb (Fig. 1A and Fig. 2A, PCR1). Cloning and sequence analysis confirmed that the 1.1- and 0.8-kb fragments encoded the α (three-loop) and β (two-loop) motifs, respectively. The 1.0-kb fragment coded for the identical translation initiation site and the first 30 NH_2-terminal residues in the 1.1- and 0.8-kb fragments. In addition, it contained a unique 144-bp substitution in place of the 267-bp sequence, which encoded the first IgG-like loop of the α motif. The 144-bp insertion was in the same reading frame as the translation initiation site and multiple stop codons, which began 94 bp downstream of the 5′ insertion site (Fig. 1). An alternate candidate translation initiation site

W. Alton Jones Cell Science Center, Inc., 10 Old Barn Road, Lake Placid, NY 12946.

*To whom correspondence should be addressed.